Magnetoplasmons in a quasi-one-dimensional quantum wire

1994 J. Phys.: Condens. Matter 6 1685

(http://iopscience.iop.org/0953-8984/6/9/011)

J. Phys.: Condens. Matter 6 (1994) 1685–1694. Printed in the UK

Magnetoplasmons in a quasi-one-dimensional quantum wire

Hui L Zhao†, Yun Zhu‡, Lihong Wang§ and Shechao Feng
Department of Physics, University of California, Los Angeles, CA 90024, USA

Received 12 July 1993, in final form 3 November 1993

Abstract. Plasmon spectra in a quasi-1D quantum wire under a transverse magnetic field are calculated within the random phase approximation (RPA) in the long-wavelength limit. We find interesting collective behaviours corresponding to the edge state electrons in both intrasubband and intersubband (between occupied subbands) excitations. The various plasmon modes show anomalous magnetic field dependences. The intrasubband and some segments of the intersubband excitation frequencies decrease with increasing field. These results are in good agreement with experiment.

1. Introduction

Plasmon excitations of a quasi-one-dimensional (quasi-1D) electron gas under a strong magnetic field have recently been studied extensively [1–3]. These elementary excitations, so-called magnetoplasmons, have become an important aspect of many-body physics and play significant roles in both integer and fractional quantum Hall effects (QHE) [4–6]. It is well known that edge states are crucial in determining transport properties of such systems [7]. As observed in [1–3], and as will be shown in this paper, magnetoplasmons are also closely associated with edge states.

Since the edge states are more significant in quasi-1D geometries, quasi-1D quantum wires provide a natural ground for studying magnetoplasmon excitations. Experimentally, the edge magnetoplasmons can be studied by inelastic scattering [1], far infrared spectroscopy [2], and radio frequency techniques [3]. Some theoretical efforts on the excitations have been reported [8]. The single-particle states in quasi-1D wires in a longitudinal magnetic field and the associated effect of the observed damping of density of states oscillations have been investigated [9]. However, the collective excitations of such systems in the presence of a *transverse* magnetic field have not been studied completely due to the difficulty of having to solve a secular equation of infinite dimensions. In [10] we proposed a general method to solve this problem, but for a quasi-1D system the problem can be solved in a rather simple way by noticing the unique feature of the 'Fermi surface' in quasi-1D geometries. Also, by varying the magnetic field strength, one can control the number of occupied subbands and study any designated collective and single-particle excitation modes. As we shall see below, in the long-wavelength limit, electrons involved in the collective excitations (except those in the intersubband excitations from occupied subbands to empty subbands) will contribute to the edge states.

† Present address: Department of Physics, University of Florida, Gainesville, FL 32611, USA.
‡ Present address: Department of Physics, University of Central Florida, Orlando, FL 32816, USA.
§ Present address: Theoretical Division, Los Alamos National Lab, Los Alamos, NM 87545, USA.

0953-8984/94/091685+10$19.50

In this paper, we study the various collective excitations in a quasi-1D quantum wire under a transverse magnetic field. Our main results can be summarized as follows. First, the applied field displaces most of the excitation modes to the edges of the quantum wire. Each intrasubband excitation has one mode that is localized on one of the two edges of the wire. The directions of the incident perturbation and the applied field determine which edge the plasmon is in. Intersubband excitations divide the wire into three regions. An intersubband excitation between occupied subbands, which was believed to be too weak to observe in the absence of a magnetic field, could be substantial in our case and has two modes with different q dependence which are localized on the two edges. The intersubband excitation between occupied and empty subbands has only one mode which is localized in the middle of the wire. Second, these magnetoplasmons show anomalous field dependences. In contrast to the bulk collective modes, whose squared frequency increases linearly with the squared cyclotron frequency, the intrasubband modes have frequencies that generally *decrease* with increasing magnetic field. If only the $n = 0$ subband is occupied (the so-called electric quantum limit), the intersubband excitation to the $n = 1$ subband has a frequency that *increases* with the applied field as we expect from conventional studies. However, for a multiple subband occupation, the intersubband excitation between occupied and empty subbands has a frequency that *decreases with the applied field due to the depopulation* effect. In contrast, the frequencies of intersubband excitations between occupied subbands *increase* with the applied field. When the subband occupation is changed by changing the applied field, one should see the transition between two modes and one mode intersubband excitations.

2. RPA in a magnetic field

We consider a quasi-1D wire with parabolic transverse confinement. The electrons are confined in the $z = 0$ plane (a standard 2D EG) and are free in the x direction. A magnetic field B is applied along the z axis. The Hamiltonian is

$$H_0 = \frac{1}{2m}\left[\left(p_x - \frac{e}{c}By\right)^2 + p_y^2\right] + \tfrac{1}{2}m\omega_0{}^2y^2. \tag{1}$$

Single-particle eigenstates and energy eigenvalues of H_0 are

$$\Psi_{nk}(x) = L^{-1/2}e^{ikx}\phi_{nk}(y) \tag{2}$$

with

$$\phi_{nk}(y) = \left(\frac{1}{2^n n!}\sqrt{\frac{\lambda}{\pi}}\right)^{1/2} H_n\left[\sqrt{\lambda}(y - y_0)\right]e^{-\lambda(y-y_0)^2/2} \tag{3}$$

$$E_{n,k} = (n + \tfrac{1}{2})\hbar\tilde{\omega} + \frac{\hbar^2k^2}{2m^*} \tag{4}$$

where H_n is a Hermite polynomial, and the parameters in (3) and (4) are

$$\begin{aligned} &\lambda = m\tilde{\omega}/\hbar \qquad y_0 = (\omega_c/\tilde{\omega})^2kl_B^2 \qquad l_B^2 = \hbar c/eB \\ &\omega_c = eB/mc \qquad \tilde{\omega}^2 = \omega_c^2 + \omega_0^2 \qquad m^* = m(\tilde{\omega}/\omega_0)^2. \end{aligned} \tag{5}$$

The effective electron mass $m \approx 0.07m_e$. Equation (3) shows that a magnetic field shifts the centre of the wavefunction towards the edge of the wire. Those states labelled by k around k_F are edge states. The corresponding energy subbands are shown in the inset in figure 1. At zero temperature, the Fermi energy and the Fermi wavenumbers $k_F^{(n)}$ associated with different subband indices n can be simply determined by

$$\begin{aligned} &\sum_{n=0} k_F^{(n)} = \pi N/2L \\ &k_F^{(n)} = \left\{2m^*[E_F - (n+1/2)\hbar\tilde{\omega}]/\hbar^2\right\}^{1/2} \end{aligned} \tag{6}$$

where N/L is the electron density of the system. To compare with experimental results, we need to relate ω_0 to the width, W, of the quantum channel. Following [11], we take $W = 2\pi(N/L)^{1/3}\left[2\hbar/(3\pi m\omega_0)\right]^{2/3}$. The full Hamiltonian of the system is $H = H_0 + H_{\text{Coulomb}}$. Using (2) as the basis for second quantization

$$H = \sum_{n,k} E_{n,k} C_{n,k}^\dagger C_{n,k} + \frac{1}{2} \sum_{\substack{kk'q \\ n_{1,2,3,4}}} V_{n_1n_2n_3n_4}(k, k', q) C_{n_1,k+q}^\dagger C_{n_2,k'-q}^\dagger C_{n_3,k'} C_{n_4,k}. \tag{7}$$

The interaction vertex is given by

$$V_{n_1n_2n_3n_4}(k, k', q) = \frac{2e^2}{\epsilon_s L} \int\int \mathrm{d}y\, \mathrm{d}y'\, \phi_{n_1,k+q}^*(y) \phi_{n_2,k'-q}^*(y') K_0(q|y - y'|) \phi_{n_3,k'}(y') \phi_{n_4,k}(y) \tag{8}$$

where $K_0(x)$ is a modified Bessel function and ϵ_s is a host dielectric constant. Let

$$\rho_{nn'kq}^\dagger = C_{n,k+q}^\dagger C_{n',k}. \tag{9}$$

Then

$$-\mathrm{i}\hbar\dot{\rho}_{nn'kq}^\dagger = [H, \rho_{nn'kq}^\dagger] = (E_{n,k+q} - E_{n',k})\rho_{nn'kq}^\dagger + [H_{\text{Coulomb}}, \rho_{nn'kq}^\dagger]. \tag{10}$$

Applying RPA to the second term in the above equation gives

$$-\mathrm{i}\hbar\langle\dot{\rho}_{nn'kq}^\dagger\rangle = (E_{n,k+q} - E_{n',k})\langle\rho_{nn'kq}^\dagger\rangle + \sum_{n_1n_4k'} (n_{n',k} - n_{n,k+q}) V_{n_1n'nn_4}(k', k+q, q)\langle\rho_{n_1n_4k'q}^\dagger\rangle \tag{11}$$

where $n_{nk} = \langle C_{n,k}^\dagger C_{n,k}\rangle$ is the average number of electrons in the subband n with momentum k. With a linear response to an external field with frequency ω

$$-\mathrm{i}\langle\dot{\rho}_{nn'kq}^\dagger\rangle = \omega\langle\rho_{nn'kq}^\dagger\rangle. \tag{12}$$

Turning off the external field, the solutions of (11) and (12) represent intrinsic excitations in the system, including plasmon excitations. Thus we need to solve

$$\langle\rho_{nn'kq}^\dagger\rangle = \sum_{mm'k'} \frac{n_{n',k} - n_{n,k+q}}{E_{n',k} - E_{n,k+q} + \hbar\omega} V_{mn'nm'}(k', k+q, q)\langle\rho_{nn'k'q}^\dagger\rangle. \tag{13}$$

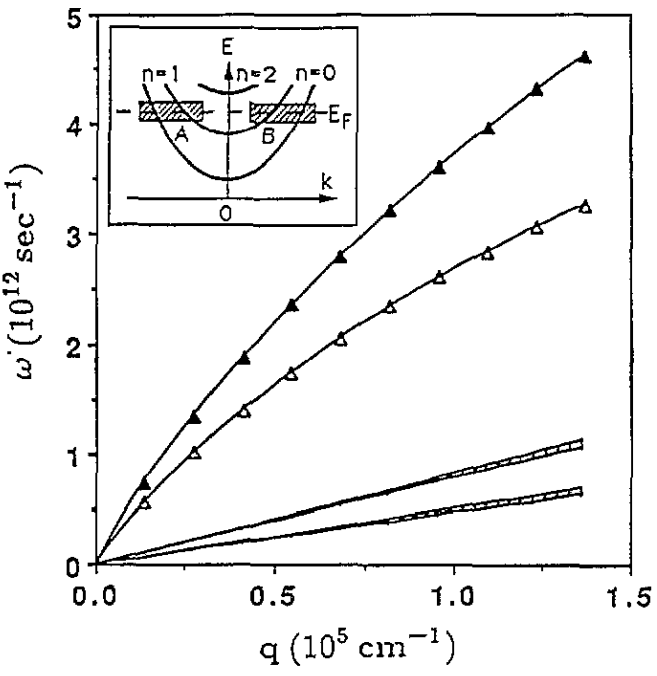

Figure 1. Intrasubband excitations in a quasi-1D quantum wire at $B = 2T$ (two subband occupation). Curves marked by ▲ and △ are the excitations in the $n = 0$ and $n = 1$ subbands, respectively. The higher and lower shaded areas are the single-particle excitation regions corresponding to the two subbands. The inset is the energy subband picture.

The difficulty in extracting the excitation frequency lies in the coupling in k' between V and ρ. In the following, we shall show that this can be avoided in the long-wavelength limit, using the peculiar property of quasi-1D Fermi surfaces (only two points, see the inset of figure 1).

Multiplying (13) by $K_0(q|y'' - y'|)\phi^*_{n,k+q}(y')\phi_{n',k}(y')$ and integrating over k and y', we obtain

$$W_{nn'q}(y'') = \frac{e^2}{\pi\epsilon_s}\sum_{mm'}\int dk\,\frac{n_{n',k} - n_{n,k+q}}{E_{n',k} - E_{n,k+q} + \hbar\omega}\int dy'\,\phi^*_{n,k+q}(y')K_0(q|y'' - y'|)\phi_{n',k}(y')$$
$$\times \int dy\,\phi_{n,k+q}(y)\phi^*_{n',k}(y)W_{mm'q}(y) \tag{14}$$

where

$$W_{nn'q}(y') = \int dy\,K_0(q|y' - y|)\sum_k \phi^*_{n,k+q}(y)\phi_{n',k}(y)\langle\rho^\dagger_{nn'kq}\rangle. \tag{15}$$

Noticing that the polarization factor in (14) is non-vanishing only around the two Fermi edges (the shaded areas A and B in the inset of figure 1), one can complete the integral over k in the long-wavelength limit ($q \ll k_F^{(n)}, k_F^{(n')}$):

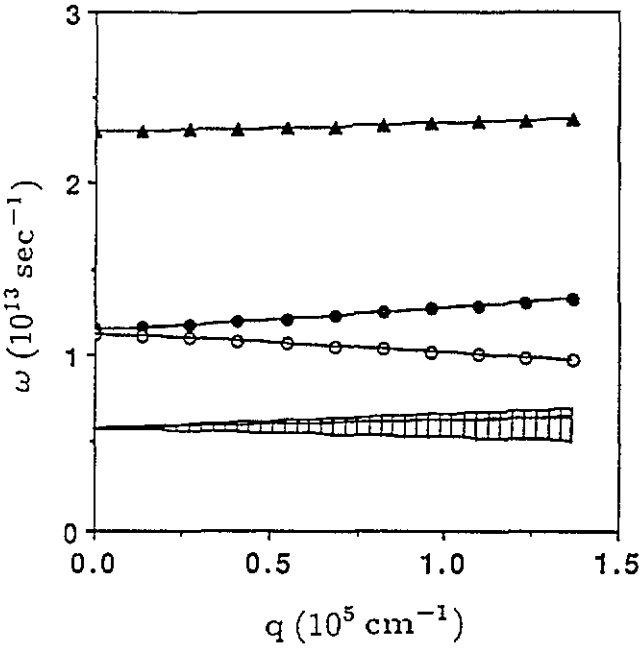

Figure 2. Intersubband excitations at $B = 2$ T. Curves marked by • and ○ are the two modes between the $n = 0$ and $n = 1$ subbands. The • mode corresponds to region B and the ○ mode corresponds to region A in the inset of figure 1. The curve marked by ▲ is the excitation between the $n = 1$ and $n = 2$ subbands. The shaded areas are the single-particle excitation regions with the higher one between the $n = 0, 1$ subbands and the lower one between the $n = 1, 2$ subbands.

$$W_{nn'q}(y'') = \frac{2e^2}{\pi\epsilon_s\hbar}\sum_{mm'}\Bigg(\Pi^{+}_{nn'}(q,\omega)\int dy'\,\phi^{*}_{n,\bar{k}_F+q}(y')K_0(q|y''-y'|)\phi_{n',\bar{k}_F}(y')$$
$$\times\int dy\,\phi_{n,\bar{k}_F+q}(y)\phi^{*}_{n',\bar{k}_F}(y)W_{mm'q}(y)$$
$$+\Pi^{-}_{nn'}(q,\omega)\int dy'\,\phi^{*}_{n,-\bar{k}_F+q}(y')K_0(q|y''-y'|)\phi_{n',-\bar{k}_F}(y')$$
$$\times\int dy\,\phi_{n,-\bar{k}_F+q}(y)\phi^{*}_{n',-\bar{k}_F}(y)W_{mm'q}(y)\Bigg) \tag{16}$$

where

$$\Pi^{\pm}_{nn'}(q,\omega) = \frac{k_F^{(n')} - k_F^{(n)} \pm q}{\omega \mp (\hbar\bar{k}_F/m^*)q + (n'-n)\tilde{\omega}} \tag{17}$$

and $\bar{k}_F = \frac{1}{2}(k_F^{(n)} + k_F^{(n')})$. Multiplying (16) by $\phi^{*}_{n',\bar{k}_F}(y'')\phi_{n,\bar{k}_F+q}(y'')$ and $\phi^{*}_{n',-\bar{k}_F}(y'')\phi_{n,-\bar{k}_F+q}(y'')$ respectively, and integrating over y'', one obtains, for non-vanishing density fluctuation, the following secular equation:

$$\begin{vmatrix} 1-\Pi^{+}_{nn'}(q,\omega)A^{+}_{nn'}(q) & -\Pi^{-}_{nn'}(q,\omega)A^{-}_{nn'}(q) \\ -\Pi^{+}_{nn'}(q,\omega)A^{-}_{nn'}(q) & 1-\Pi^{-}_{nn'}(q,\omega)A^{+}_{nn'}(q) \end{vmatrix} = 0 \tag{18}$$

where, noticing that ϕ are real,

$$A^{\pm}_{nn'}(q) = \frac{2e^2}{\pi\epsilon_s\hbar}\int\int \mathrm{d}y\,\mathrm{d}y'\,\phi_{n,\bar{k}_F+q}(y')\phi_{n',\bar{k}_F}(y')K_0(q|y-y'|)\phi_{n,\pm\bar{k}_F+q}(y)\phi_{n',\pm\bar{k}_F}(y). \tag{19}$$

In doing this, we have neglected the coupling between the subbands, n, n', and others (terms with $m \neq n$ and $m' \neq n'$ are generally smaller because of the orthogonality of base wavefunctions). To simplify our notation, we write $A_1(q) = A^{+}_{nn'}(q)$ and $A_2(q) = A^{-}_{nn'}(q)$. The solution of (18) is

$$\omega = (n-n')\tilde{\omega} + (k_F^{(n')} - k_F^{(n)})A_1(q) \pm \left\{\left[A_1^2(q) - A_2^2(q) + 2A_1(q)\frac{\hbar\bar{k}_F}{m^*} + \left(\frac{\hbar\bar{k}_F}{m^*}\right)^2\right]q^2 + A_2^2(q)\left(k_F^{(n')} - k_F^{(n)}\right)^2\right\}^{1/2}. \tag{20}$$

Equation (20) is the magnetoplasmon frequency for *intrasubband* excitations when $n = n'$, and for *intersubband* excitations between *occupied* subbands when $n > n'$. For the intersubband excitation from an *occupied* subband (n') to an *empty* subband (n), the approximation we used in evaluating the integral over k in (14) is not valid. In this case, only *one* Fermi distribution function appears in (14), which implies that *all* electrons in the subband n' are involved in the excitation to the empty subband n. One can give a rough estimate of the excitation frequency in the long-wavelength limit ($k_F^{(n')}q \ll m^*\tilde{\omega}$) by evaluating the integral in (14) with $k = \bar{k}_F = k_F^{(n')}/2$ in the integrand. This gives

$$\omega \approx (n-n')\tilde{\omega} + 2A_1(q)k_F^{(n')}. \tag{21}$$

Numerically calculated dispersion curves are shown in figures 1 and 2. The various parameters were chosen for a typical quasi-1D quantum wire cut from GaAs/$Al_xGa_{1-x}As$, with $W \sim 0.1\,\mu$m, $N/L \sim 2.3 \times 10^6\,\mathrm{cm}^{-1}$ ($\hbar\omega_0 \approx 1.77$ meV) and $\epsilon_s \sim 13$. We take the magnetic field to be $B = 2$ T ($\hbar\omega_c \approx 3.3$ meV), at which the two subbands are occupied. We then obtain $k_F^{(0)} \approx 2.24 \times 10^6\,\mathrm{cm}^{-1}$, $k_F^{(1)} \approx 1.36 \times 10^6\,\mathrm{cm}^{-1}$ and $E_F \approx 2.09\hbar\tilde{\omega} \approx 7.8$ meV. The intrasubband excitations (for subbands 0 and 1) and the intersubband excitation between the two subbands are calculated by (20). The intersubband excitation mode between $n' = 1$ and $n = 2$ is calculated from (21). The single-particle excitation regions (shaded area), where plasmon excitations are damped, are determined by the condition that the imaginary part of (14) is finite when replacing ω by $\omega + \mathrm{i}\eta$ and letting $\eta \to 0$, i.e.

$$\lim_{\eta\to 0} \mathrm{Im}\sum_k \frac{n_{n',k} - n_{n,k+q}}{E_{n',k} - E_{n,k+q} + \hbar\omega + \mathrm{i}\eta} \neq 0 \tag{22}$$

which gives

$$\frac{\hbar}{2m^*}k_F^{(n)}q < \omega < \frac{\hbar}{2m^*}(k_F^{(n)}q + q^2) \tag{23}$$

for intrasubband excitations and

$$(n-n')\tilde{\omega} + \frac{\hbar}{2m^*}k_F^{(n)}q < \omega < (n-n')\tilde{\omega} + \frac{\hbar}{2m^*}(k_F^{(n')}q + q^2) \tag{24}$$

for intersubband excitations from n' to n.

3. Discussion

We now discuss, in physical terms, the following three features of the dispersion curves.

(i) Intrasubband excitations ($n = n'$) show an acoustic-like dispersion as $q \to 0$. The leading term of the excitation mode of the nth subband, as $q \to 0$, scales as

$$\omega \approx \left(\frac{\hbar k_F^{(n)} c}{137\epsilon_s m^*}\right)^{1/2} q[\ln(q_0/q)]^{1/2} \tag{25}$$

with $q_0 \sim \sqrt{\lambda}$, the inverse of the wire width. Notice that the coefficient in front of q decreases with increasing field. Since $k_F^{(n)} < k_F^{(n')}$ for $n > n'$, the excitation frequency becomes smaller for subbands with higher indices n, as shown in figure 1. In the long-wavelength limit (small q), intrasubband modes can be excited only around one of the two Fermi edges (regions A or B in the inset to figure 1). For $q > 0$, there are states available in region B for intrasubband excitation, but no intrasubband excitation can be detected in region A since all destination states are occupied. In the presence of a magnetic field, the states around Fermi edges are displaced to the two edges of the quantum wire, states around $+k_F^{(n)}$ to the upper edge ($y > 0$ side) and states around $-k_F^{(n)}$ to the lower edge ($y < 0$ side), i.e. the edge states [7]. Therefore, by applying a magnetic field perpendicular to the wire, a spatial *asymmetry* is introduced. For $q > 0$, the intrasubband excitations will appear at the upper edge ($y > 0$) of the wire, while no intrasubband excitation occurs at the lower edge ($y < 0$). Changing the sign of q or the field direction reverses the spatial distribution of these excitations so that the intrasubband modes will appear at the lower edge of the quantum wire.

(ii) For intersubband excitations between occupied subbands with $n' > n$, both solutions in (20) are negative and should be discarded. For $n' < n$, however, we obtain *two* solutions corresponding to the two Fermi edges. The two modes between the subbands $n = 0, 1$ have different q dependences; one increases with q, the other decreases with q. This can also be understood physically from the inset of figure 1. As $q \to 0$, we obtain

$$\omega \approx \tilde{\omega} + (A_1 \pm A_2)(k_F^{(0)} - k_F^{(1)}) \tag{26}$$

which confirms that only electrons in regions A and B in the $n = 0$ subband are involved in excitation between the $n = 0$ and $n = 1$ subbands. The gap at $q = 0$ is due to the coupling between the upper-edge mode and the lower-edge mode. Both the frequency and intensity [12] of an intersubband excitation depends sensitively on the number of electrons involved in the excitation, namely the more electrons participate in the excitation, the higher are the excitation frequency and intensity. For intersubband excitation between the $n = 1, 2$ (occupied and empty) subbands, as we see from the inset of figure 1, all electrons in the $n = 1$ subband are involved in excitation from the $n = 1$ to $n = 2$ subbands. As $q \to 0$, we obtain from (21)

$$\omega \approx \tilde{\omega} + \gamma \frac{c k_F^{(1)}}{137\epsilon_s} \tag{27}$$

with γ being a constant of order unity. From these discussions we see that, in the presence of a magnetic field, the electrons participating in intersubband excitations are effectively divided into *three* spatially separated parts for the case of two subband occupation, namely those at the two Fermi edges of the $n = 0$ subband (with density $\sim k_F^{(0)} - k_F^{(1)}$) and

those of the $n = 1$ subband (with density $\sim k_F^{(1)}$). If the applied field is adjusted so that $k_F^{(0)} \approx 2 \sim 3k_F^{(1)}$, i.e. the number of electrons involved in the three intersubband modes are comparable, one should be able to see all *three* intersubband modes. Here we emphasize the importance of the parabolic confining potential of the quantum wire. If the potential is flattened over a large region inside the wire, then the electrons involved in intersubband excitations between occupied subbands (e.g. $n = 0, 1$) will be much less than those involved in intersubband excitation between occupied and empty subbands (e.g. $n = 1, 2$). In this case, the intersubband mode between the last filled subband and the first empty subband will dominate the excitation spectra, since the intensities of the other intersubband modes are much smaller. For quasi-1D quantum wires obtained on a split-gate GaAs/$Al_xGa_{1-x}As$ heterojunction, it has been shown that the gate voltage can actually change the effective potential between a parabolic and a flattened potential profile [13].

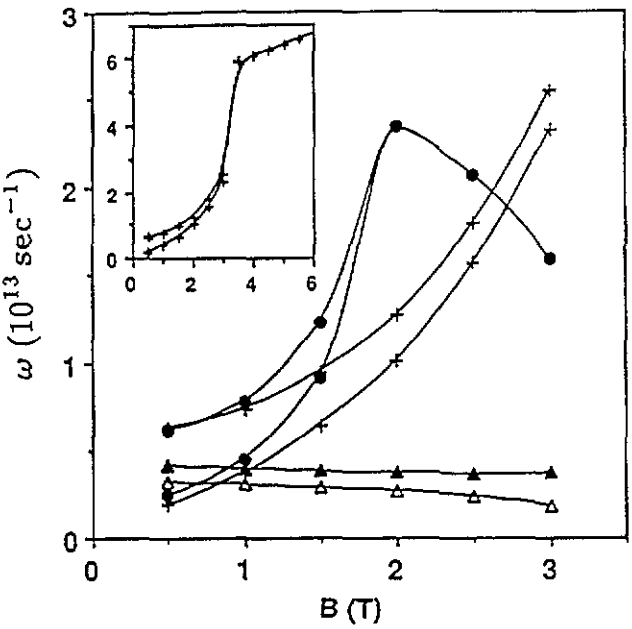

Figure 3. Field dependence of excitation frequencies at $q = 10^5\,cm^{-1}$. Curves marked by ▲ and △ are the intrasubband excitations in the $n = 0$ and $n = 1$ subbands, respectively. Curves marked by + are the two modes between the $n = 0$ and $n = 1$ subbands. Curves marked by • are the intersubband excitation between the $n = 1$ and $n = 2$ subbands. The inset is the dependence of the excitation frequency between the $n = 0$ and $n = 1$ subbands on the magnetic field over a wider range.

(iii) Figure 3 shows the magnetic field dependence of the various excitation modes at $q = 10^5\,cm^{-1}$. The intrasubband frequencies are not very sensitive to the field variation; they generally show a decreasing tendency with increasing B, in agreement with the edge magnetoplasmons calculated previously from a hydrodynamic model [14]. Such behaviours have been verified by experiments in [2]. The intersubband excitation frequencies between occupied subbands ($n = 0, 1$) increase with the field due to the increase of $\tilde{\omega}$, as seen from (26). The intersubband excitation between occupied and empty subbands ($n = 1, 2$) decreases with increasing field as a result of the depopulation effect (reduction in $k_F^{(1)}$) from

the $n = 1$ subband, which dominates in (27). This single intersubband mode will split into two modes when the field is sufficiently lowered such that the $n = 2$ subband starts to be occupied. The split modes show a similar field dependence as the intersubband modes between the $n = 0, 1$ subbands. The inset in figure 3 shows the field dependence of the intersubband excitation from $n = 0$ to $n = 1$ in a wider field range. Again there is only one mode when the field is increased so that the $n = 1$ subband becomes completely depleted. But this single mode increases with increasing field, in contrast to that from the $n = 1$ to $n = 2$ mode. This is because there is no depopulation effect in the $n = 0$ subband, while $\tilde{\omega}$ increases with increasing field. Changing the electron density in the system while fixing the magnetic field would have the same effect as fixing the electron density while decreasing the applied field for a multiple subband occupation. We expect that the curves of frequency against electron density will be similar to figure 3. Nevertheless the degenerate mode in the inset of figure 3 will increase with increasing electron density (thus increasing $k_F^{(0)}$), so that curves in the new inset will be similar to those between the $n = 1, 2$ subbands.

We conclude by briefly discussing the experimental situation. Both intrasubband and intersubband plasmon excitations have been observed experimentally. Dispersion curves calculated here are similar to those observed in the absence of a magnetic field [1], i.e. the intrasubband excitation frequency grows like $q(\ln q)^{1/2}$ and the intersubband excitation frequency shows almost no dependence on q. Complete dispersion curves in the presence of magnetic fields are still not available. Perhaps more interesting is the field dependence of excitation frequencies. Contrary to intuition, the intrasubband plasmon frequency decreases with increasing field. This behaviour has been observed in experiment [2]. The intersubband plasmon frequency were found to increase with the applied field [1, 2]. The decreasing intersubband branch in figure 3 was not observed. Probably this is because it has an energy higher than those accessible by the far-infrared radiation technique. However, there are traces of the depopulation effect in [2], i.e. one intersubband mode disappeared as the field increased.

Acknowledgments

We wish to thank D C Tsui, B L Altshuler and S Das Sarma for valuable discussions. This work was supported in part by a grant from the DOE under grant number DE-FG03-88ER45378.

References

[1] Goñi A R, Pinczuk A, Weiner J S, Calleja J M, Dennis B S, Pfeiffer L N and West K W 1993 *Phys. Rev. Lett.* **70** 1151; 1991 *Phys. Rev. Lett.* **67** 3298

[2] Demel T, Heitmann D, Grambow P and Ploog K 1991 *Phys. Rev. Lett.* **66** 2657; 1988 *Phys. Rev.* B **38** 12732

[3] Wassermeier M, Oshinowo J, Kotthaus J P, MacDonald A H, Foxon C T and Harris J J 1990 *Phys. Rev.* B **41** 10287

[4] Saitoh M (ed) 1992 *Proc. 9th Int. Conf. on Electronic Properties of 2D Systems (Nara, Japan, 1991); Surf. Sci.* **263**

[5] Girvin S 1987 *The Quantum Hall Effect* ed R Prange and S Girvin (Berlin: Springer)

[6] Lee D H and Zhang S C 1991 *Phys. Rev. Lett.* **66** 1220

[7] Halperin B I 1982 *Phys. Rev.* B **25** 2185
MacDonald A H and Středa P 1984 *Phys. Rev.* B **29** 1616
Büttiker M 1988 *Phys. Rev.* B **38** 9375

[8] Li Q P and Das Sarma S 1991 *Phys. Rev.* B **43** 11768; **44** 6277
[9] Smith T P III, Brum J A, Hong J A, Knoedler C M, Arnot H and Esaki L 1988 *Phys. Rev. Lett.* **61** 585
Zhao H L, Zhu Y and Feng S 1989 *Phys. Rev.* B **40** 8107
[10] Wang L, Zhu Y, Zeng F, Zhao H L and Feng S 1993 *Phys. Rev.* B **47** 16326
[11] Berggren K F, Roos G and van Houten H 1988 *Phys. Rev.* B **37** 10118
[12] Jain J K and Allen P B 1985 *Phys. Rev.* B **32** 997
Hawrylak P, Wu J W and Quinn J J 1985 *Phys. Rev.* B **32** 5169
[13] Laux S E, Frank D J and Stern F 1988 *Surf. Sci.* **196** 101
[14] Fetter A L 1986 *Phys. Rev.* B **33** 3717